Materials Science Forum
ISSN: 1662-9752, Vol. 890, pp 223-226
doi:10.4028/www.scientific.net/MSF.890.223

Submitted: 2016-11-08
Accepted: 2016-11-17
Online: 2017-03-20

Photon-Induced L-Shell X-Ray Production Cross Sections for Lanthanides at 59.54 keV

Rıdvan Durak[1,a], Ferdi Akman[2,b] and Abdulhalik Karabulut[3,c]

[1]Atatürk University, Science Faculty, Department of Physics, Erzurum, 25240, Turkey

[2]Bingöl University, Vocational School of Technical Sciences, Department of Electronic Communication Technology, Bingöl, 12000, Turkey

[3]Atatürk University, Science Faculty, Department of Physics, Erzurum, 25240, Turkey

[a]rdurak@atauni.edu.tr, [b]fakman@bingol.edu.tr, [c]akara@atauni.edu.tr

Keywords: L shell; X-ray production cross section; Photon-induced; X-ray fluorescence

Abstract. The Ll, Lα and Lβ X-ray production cross sections for Pr, Nd, Sm, Eu, Gd and Tb elements were determined using a reflection geometry. The excitation was performed with a ^{241}Am radioactive annular source and the L X-rays emitted from targets were counted with a high-resolution Si(Li) detector. The experimental values were compared with other available experimental results and theoretical data. An agreement is observed between the measured and other experimental results or theoretical data.

Introduction

The determinations of X-ray production (XRP) cross section, fluorescence yield, intensity ratio and vacancy transfer probability are very crucial to grasp the ionization of atom. The accurate data on these parameters are required for some basic studies such as non-destructive and trace-element analysis in archaeological, biological, medical, industrial applications; dosimetric computations and cancer therapy for health physics; radiation shielding, environmental and material science applications.

Many workers and work groups determined the L shell X-ray production cross sections by photons or protons at different excitation energies [1-11]. Bendjedi et al. [1] compiled X-ray production cross sections for a wide range of elements by proton impact up to 10 MeV. The Ll, Lα, Lβ and Lγ X-ray production cross sections for Yb, Ta, W, Hg, Tl, Pb, Bi, Th and U [2]; for Ho, Lu, W, Hg and Bi [3]; for Sm, Eu, Gd, Dy, Ho, Er, Pt, Au, Tl, Pb and Bi [4]; and for some selected elements between Caesium and Erbium [5] were determined at 59.54 keV photon energy emitted from a ^{241}Am source. The X-ray production cross sections of different L sub-shell for six elements with $56 \leq Z \leq 68$ [6] and for some elements in the atomic range $66 \leq Z \leq 92$ [7] were obtained at 22.6 keV photon energy emitted from a ^{109}Cd radioactive source. The Ll, Lα, $L\beta_1$, $L\beta_2$, $L\gamma_1$ and $L\gamma_2$ XRP cross sections for elements with $45 \leq Z \leq 50$ at 9 keV [8]; the Lα, Lβ and Lγ XRP cross sections for some selected elements between La and Lu at 15.2 keV [9]; and the Ll, Lα, Lβ and Lγ XRP cross sections for fourteen elements in the atomic number range $55 \leq Z \leq 81$ at 15.73 keV [10] were measured using the different types of radioactive sources. The Ll, Lα, Lβ and Lγ XRP cross sections for five elements with $62 \leq Z \leq 70$ were estimated by Mandal et al. [11] at 17.8, 22.6 and 25.8 keV energies using an X-ray tube and secondary exciters.

In the present work, the Lα, Lβ and Lγ X-ray production cross sections for Pr, Nd, Sm, Eu, Gd and Tb elements were measured using a reflection experimental set-up at 59.54 keV photon energy emitted from a ^{241}Am annular radioactive source and a high-resolution Si(Li) detector. The measured results were compared with the theoretical and other available experimental results. Within the experimental uncertainties, the measured results agree with the theoretical values and other available values.

Experimental and calculation procedure

The experiments were performed using the reflection experimental geometry as shown in Fig. 1. A sandwich filter made from Pb, Fe and Al was used to protect the detector from other undesired radiation and to minimize the background counts. The L X-ray line intensities from the target were counted with a high-resolution Si(Li) detector which has 12.5 mm^2 active area, 0.008 mm thickness Be window and 160 eV resolution at 5.96 keV coupled to a counting system consisting of preamplifier, amplifier, analog digital converter and 4096 multi-channel analyzer interfered with a personal computer supplied with Maestro software for data acquisition.

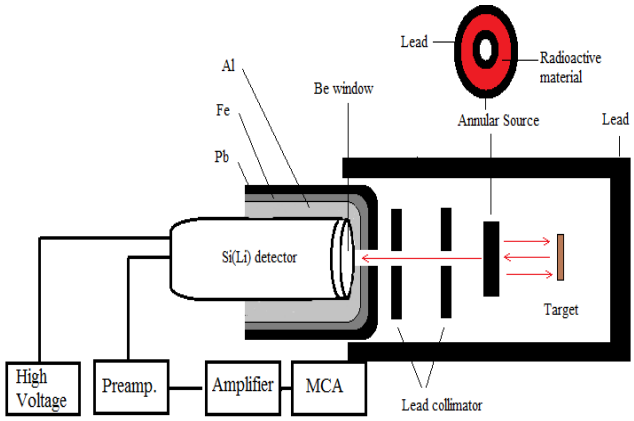

Fig. 1 Experimental set-up

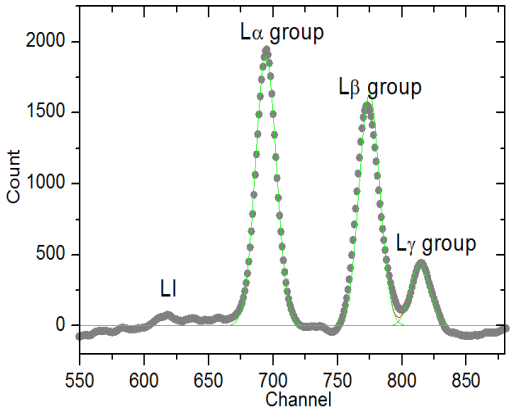

Fig. 2 Typical L X-ray spectrum of Tb at 59.54 keV

The samples were placed at 45° angles with respect to the direct beam and fluorescent X-rays were emitted at 0°. Disc samples with 20 mm diameter were prepared with the aid of pellet dies and a manual hydraulic press. The mass thicknesses of samples were obtained ranging from 0.090-0.371 g/cm^2. Each sample was excited and counted during time intervals ranging from 72000 to 86400 s to obtain the statistical accuracy. A sealed annular radioactive source of ^{241}Am (about 100 mCi) was used as the excitation source. The l X-ray line peaks were evaluated with the nonlinear least squares method and fitted with multi-Gaussian function with the help of Microcal Origin 7.5 software program. A typical L X-ray spectrum of Tb sample is shown in Fig. 2.

The L shell XRP cross sections were obtained experimentally using the relation,

$$\sigma_{Li} = \frac{A}{N}\frac{N_{Li}}{I_0 G \varepsilon_{Li} \beta_{Li} t} \quad (i = l, \alpha, \beta) \tag{1}$$

where, A is the atomic weight, N is the Avogadro number, N_{Li} is the number of counts per second under the L_i photo-peak, I_o is the incident radiation flux coming from the source, G is the geometry factor between the detector and the sample, ε is the detector efficiency, t is the mass per unit area, β is the self-absorption correction factor and it can be determined using the relation,

$$\beta = \left(1 - exp\left\{-\left[\frac{(\mu/\rho)_i}{cos\theta_1} + \frac{(\mu/\rho)_e}{cos\theta_2}\right]t\right\}\right)\left\{\left[\frac{(\mu/\rho)_i}{cos\theta_1} + \frac{(\mu/\rho)_e}{cos\theta_2}\right]t\right\}^{-1} \tag{2}$$

where, $(\mu/\rho)_i$ and $(\mu/\rho)_e$ are the total mass attenuation coefficients of the incident and emitted X-rays taken from WinXCOM [12], θ_1 and θ_2 are the incident and emitted angles of the X-rays.

The $I_0G\varepsilon$ values which includes the incident flux, geometry factor and detector efficieny were determined utilizing the relation very similar to Eq. 1 but valid for K X-rays instead of L_i X-rays. The $I_0G\varepsilon$ values were obtained by collecting the Kα and Kβ X-rays spectra of Ti, V, Cr, Mn, Fe, Co, Ni, Cu, Zn, Se and Y elements in the same experimental geometry.

$$I_0 G \varepsilon_{Ki} = \frac{A}{N} \frac{N_{Ki}}{\sigma_{Ki} \beta_{Ki} t} \quad (i = \alpha, \beta) \tag{3}$$

where, all terms are same in Eq. 1 but for K X-rays instead of the L X-rays and the theoretical values of σ_{Ki} were calculated using the relation,

$$\sigma_{Ki} = \sigma_K(E) \omega_K F_{Ki} \tag{4}$$

where, $\sigma_K(E)$ is the K shell photo-ionization cross section [13] at given energy, ω_K is the K shell fluorescence yield [14] and F_{Ki} is the fractional emission rate for K_i X-ray and was determined by,

$$F_{K\alpha} = \left(1 + \frac{I_{K\beta}}{I_{K\alpha}}\right)^{-1} \qquad F_{K\beta} = \left(1 + \frac{I_{K\alpha}}{I_{K\beta}}\right)^{-1} \tag{5}$$

where, $I_{K\beta}/I_{K\alpha}$ is the Kβ to Kα X-ray intensity ratio [15]. The measured $I_0 G\varepsilon$ values for the present experimental geometry were plotted as a function of energy in Fig. 3. The calculation process of theoretical L_i X-ray production cross sections has been described elsewhere [2,5].

Results and discussion

The L_i X-ray production cross sections were obtained using the Eq. 1. The measured value of Ll, Lα and Lβ X-ray production cross sections for Pr, Nd, Sm, Eu, Gd and Tb elements at 59.54 keV photon energy are listed in Table 1 along with the theoretical calculation values and other available experimental results. The unit of all X-ray production cross sections is barns/atom.

Table 1 Experimental and theoretical values of Lι, Lα and Lβ X-ray production cross sections at 59.54 keV photon energy

	Li X-ray production cross section (barns/atom)								
	Ll			Lα			Lβ		
Atomic Number	Exp.	Theo.	Other Exp.	Exp.	Theo.	Other Exp.	Exp.	Theor.	Other Exp.
59	-	4.69	4.8±0.4[5]	124.26±8.68	118.62	123.2±7.7[5]	91.78±6.19	95.26	97.9±6.1[5]
60	-	5.27	5.5±0.4[5]	133.99±8.39	132.59	139.1±9.3[5]	99.66±6.11	106.64	105.9±7.3[5]
62	6.63±0.30	6.07	6.8±0.5[5]	140.73±4.58	149.70	168.92±11.13[4]	117.34±3.58	124.97	135.11±9.67[4]
63	8.23±0.34	7.36	-	176.40±6.63	179.87	188.91±12.56[4]	145.14±10.04	149.43	152.25±11.11[4]
64	8.80±0.49	8.18	-	209.78±6.69	197.78	206.80±13.80[4]	156.70±9.22	166.60	173.41±12.77[4]
65	9.14±0.62	9.15	9.4±0.4[5]	203.84±6.15	218.73	229.4±10.2[5]	171.80±9.06	184.77	191.5±8.5[5]

In the determination of Ll, Lα and Lβ X-ray production cross sections, the uncertainties were estimated o be 4.13-6.78%, 3.02-6.99% and 3.05-6.74%, respectively. These uncertainties are the quadrature sum of uncertainties of evaluation of L_i X-ray peak areas, mass per unit areas, detector efficiencies, self-absorption correction factors and systematic uncertainties.

To facility comprehensive analysis, the measured and theoretical values of L_i X-ray production cross section are plotted as a function of atomic number in Fig. 4. As seen from Table 1 and Fig. 4, the L_i X-ray production cross section values increase with increasing atomic number, namely, the L_i X-ray production cross section shows a positive correlation with atomic number. The differences between the measured with the theoretical results are 0.11-11.82% for Ll XRP cross sections, 1.06-6.81% for Lα XRP crosssections and 2.87-7.02% for Lβ XRP cross sections. The maximum differences between our measured results to other available experimental results are found to be 2.77% for Ll XRP cross sections, 11.14% for Lα XRP cross sections (except Sm) and 13.15% for Lβ XRP cross sections. Table 1 and Fig. 4 show that the experimental values of L_i X-ray production cross section are generally in good agreement with the theoretical predictions and other available experimental results within experimental standard deviations.

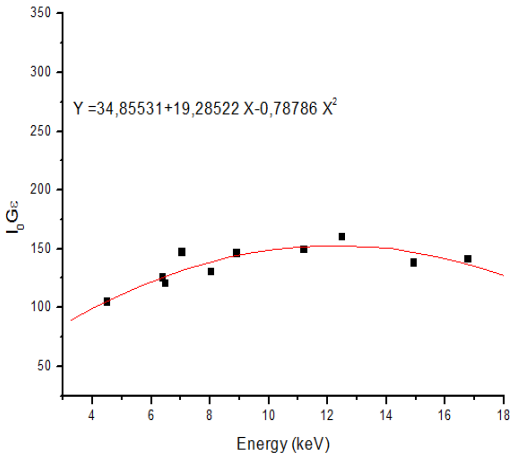

Fig. 3 $I_0 G\varepsilon$ versus energy

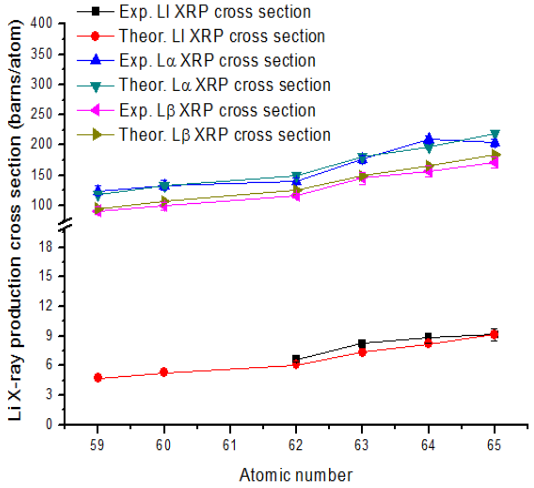

Fig. 4 L_i X-ray production cross section versus atomic number

The present agreement between the experimental and the theoretical results or other available experimental results leads to the decision that this method will be reliable for estimation the L_i X-ray production cross sections.

Acknowledgements

The authors wish to thank Atatürk University Research Fund under project no. 2011/82 for financial support.

References

[1] A. Bendjedi, B. Deghfel, A. Kahoul, I. Derradj, F. Khalfallah, Y. Sahnoune, A. Bentabet and M. Nekkab: Radiat. Phys. Chem. 117 (2015), 128.

[2] F. Akman, R. Durak, M.R. Kaçal and M.F. turhan: Can. J. Phys. 93 (2015), 1057.

[3] M.F. Turhan, R. Durak and F. Akman: Appl. Radiat. Isot. 89 (2014), 151.

[4] I. Han, L. Demir and M. Ağbaba: Radiat. Phys. Chem. 76 (2007), 1551.

[5] R. Durak and Y. Özdemir: Spectrochim. Acta B 55 (2000), 177.

[6] Y. Chauhan, M.K. Tiwari and S. Puri: Nucl. Instrum. Method B 266 (2008), 30.

[7] M.R. Kaçal, R. Durak, F. Akman, M.F. Turhan and I. Han: radiat. Phys. Chem. 80 (2011), 692.

[8] E.V. Bonzi, N.M. Badiger, G.B. Grad, R.A. Barrea and R.G. Figueroa: Appl. Radiat. Isot. 70 (2012), 632.

[9] W. Salah and J. Al-Jundi: J. Quant. Spec. Radiat. Trans. 94 (2005), 325.

[10] A. Kaya and M. Ertuğrul: J. Electron Spectrosc. 130 (2003), 111.

[11] A.C. Mandal, S. Santra, D. Mitra, M. Sarkar and D. Bhattacharya: Nucl. Instrum. Method B 234 (2005), 176.

[12] L. Gerward, N. Guilbert, K. Bjorn and H. Levring: Radiat. Phys. Chem. 60 (2001), 23.

[13] J.H. Scofield: UCRL Report 51326, Lawrence Livermore Laboratory, Livermore, CA, 1973.

[14] M.O. Krause: J. Phys. Chem. Ref. Data 8 (1979), 307.

[15] J.H. Scofield: At. Data Nucl. Data Tables 14 (1974), 121.